An introduction to Quasielastic Neutron Scattering (QENS)

John R. D. Copley
(jcopley@nist.gov)
NIST Center for Neutron Research

Outline

- A brief history of neutron scattering
- Scattering fundamentals
- What is QENS, and what does it look like?
- How is QENS measured?
- How is QENS modeled?
- Practicalities
- Examples of QENS
- Further reading
- The bottom line

A brief history of neutron scattering

- Diffraction --- Shull and Wollan (late ’40s)

The original two axis spectrometer at the “Clinton Pile”, Oak Ridge (critical 1943)

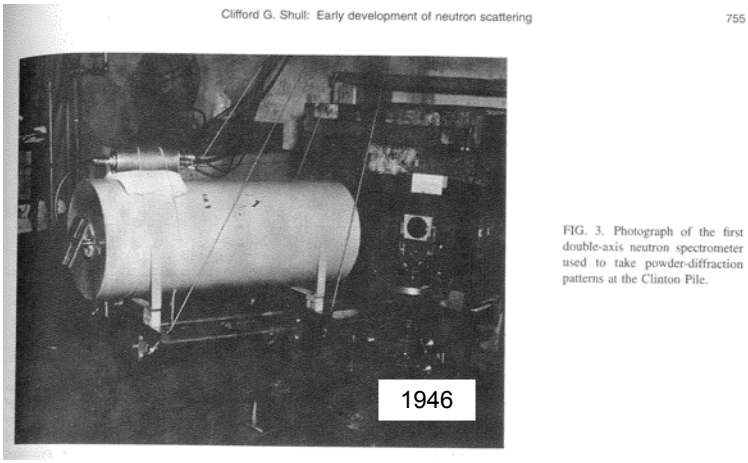

FIG. 3. Photograph of the first double-axis neutron spectrometer used to take powder-diffraction patterns at the Clinton Pile.

C.G. Shull, Rev. Mod. Phys. 67 (4) 753 (1995)
[Nobel lectures in physics 1994]

Neutron diffractometer at the Graphite Reactor (Clinton Pile), ORNL

E.O. Wollan C.G. Shull

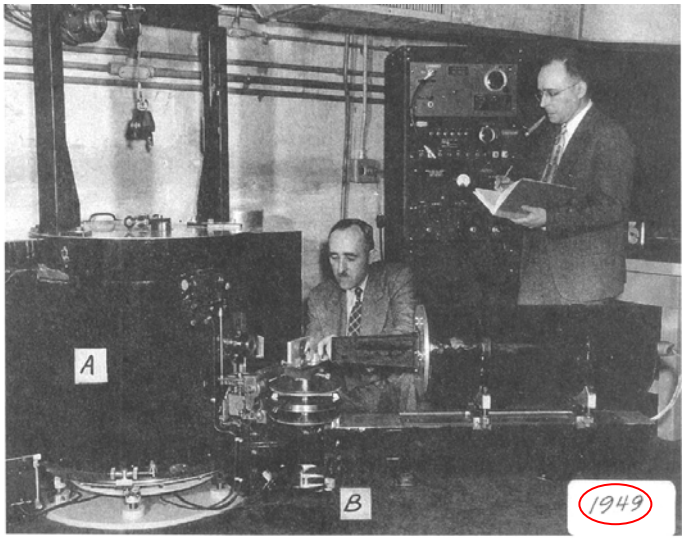

C.G. Shull, Rev. Mod. Phys. 67 (4) 753 (1995)

A brief history of neutron scattering

- Diffraction --- Shull and Wollan (late ’40s)
- Inelastic scattering --- Brockhouse (’50s)
  - Absorbers
  - Triple axis, time-of-flight

Triple axis spectrometer at NRX reactor, Chalk River, 1954

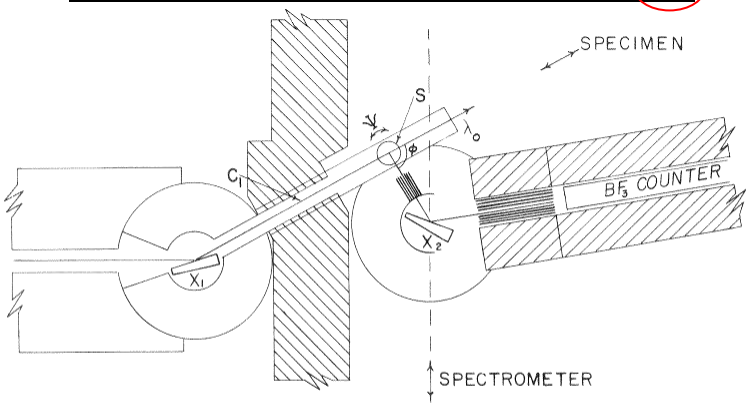

THE FIRST TRIPLE-AXIS CRYSTAL SPECTROMETER AT CHALK RIVER AT NRX REACTOR BUILT BY B.N. BROCKHOUSE IN 1954. NEUTRONS FROM THE REACTOR TO THE LEFT OF THE PICTURE ARE BRAGG SCATTERED BY A FANKUCHEN CUT MONOCHROMATOR. THIS ALUMINUM CRYSTAL IS MOUNTED AS THE ANALYSING CRYSTAL IN APPARATUS EXHIBITED.

B.N. Brockhouse, Rev. Mod. Phys. 67 (4) 735 (1995) [Nobel lectures in physics 1994]

Neutron diffractometer at the NRX reactor, Chalk River (critical 1947)

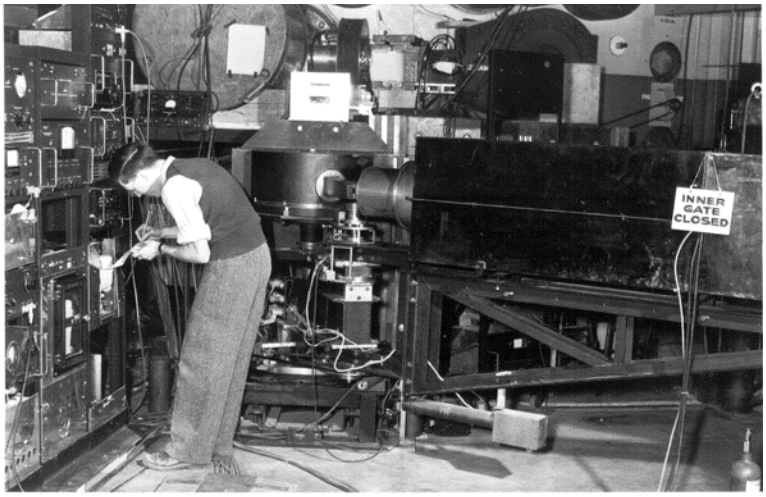

Courtesy
W.J.L. Buyers

NEUTRON DIFFRACTION APPARATUS BUILT IN THE LATE FORTIES AT NRX REACTOR BY D.G. HURST WHO STARTED NEUTRON SCATTERING AT CHALK RIVER. N.Z. ALCOCK IS SHOWN READING A CHART. NOTE THE MODEST MONOCHROMATOR SHIELD AND HUGE DETECTOR SHIELD.

A brief history of neutron scattering

- Diffraction --- Shull and Wollan (late '40s)
- Inelastic scattering --- Brockhouse ('50s)
  - Absorbers
  - Triple axis, time-of-flight
  - Phonons, spin waves, liquids, …

MINUTES OF THE 1955 ANNUAL MEETING HELD AT NEW YORK CITY, JANUARY 27–29, 1955

(Corresponding to *Bulletin of the American Physical Society*, Volume 30, No. 1)

M7. Slow Neutron Spectrometry—A New Tool for the Study of Energy Levels in Condensed Systems. B. N. BROCKHOUSE, *Chalk River Laboratories.*—It has long been realized that energy distributions of initially monoenergetic neutrons scattered by molecules or condensed systems would yield important information not otherwise easily accessible to experiment. With high reactor flux and suitable spectrometer design such measurements are now feasible. Monoenergetic neutrons, selected from the *NRX* reactor spectrum by a crystal, are scattered by the specimen and the energy distribution of the scattered neutrons is analyzed by another crystal. A survey of the field has been made and more detailed studies are in progress. The sharp division of incoherent scattering into elastic and inelastic components predicted by theory has been verified with vanadium. In liquid lead, light water, and heavy water a similar division into a "quasi-elastic" component, and an inelastic component which increases with increasing angle, can be made. For coherent scattering the "elastic" component is associated with the peaks in the liquid diffraction pattern. In liquid lead the inelastic component is similar to that of the solid at about the same temperature and angle of scattering. Diffuse magnetic scattering, studied with MnO and Mn_2O_3, and with Cr_2O_3 above and below its Néel temperature, is largely inelastic, the mean energy changes being of the order of the Néel temperatures.

Invited Paper

M8. Study of Energy Levels in Solids, Liquids, and Magnetic Materials by Scattered Slow Neutrons. B. N. BROCKHOUSE, *Chalk River Laboratories.* (30 min.)

Structural Dynamics of Water by Neutron Spectrometry (*).

B. N. BROCKHOUSE

General Physics Branch, Atomic Energy of Canada Limited - Chalk River, Ontario

Suppl. Nuovo Cimento
9, 45 (1958)

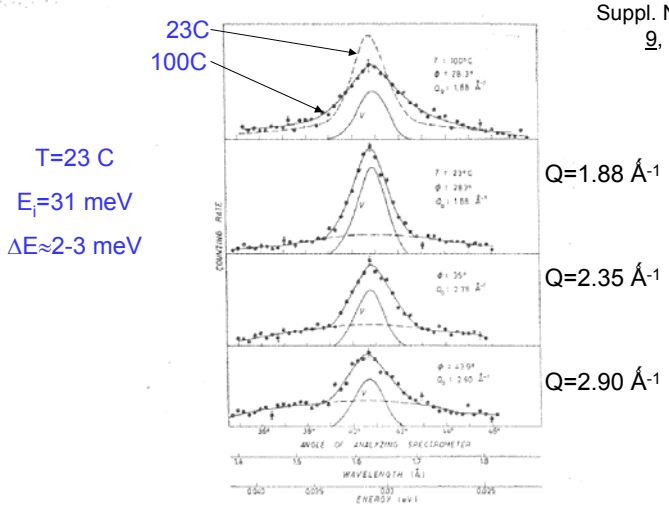

A brief history of neutron scattering

- Diffraction --- Shull and Wollan (late ’40s)
- Inelastic scattering --- Brockhouse (’50s)
  - Absorbers
  - Triple axis, time-of-flight
  - Phonons, spin waves, liquids, …
- High resolution instruments, high flux reactors (’60s, ’70s),…
- **USERS**: chemists, biologists, etc etc

Scattering fundamentals

Elastic and inelastic scattering

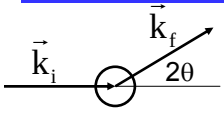

$$\hbar\omega = E_i - E_f \qquad \vec{Q} = \vec{k}_i - \vec{k}_f$$

1 meV ≈ 0.24×10^{12} c/s
8.1 cm^{-1}
11.6K
0.023 kcal/mol
0.10 kJ/mol

Coherent and incoherent scattering

$$\sigma_{coh} = 4\pi\langle b\rangle^2 \qquad \sigma_{inc} = 4\pi\left(\langle b^2\rangle - \langle b\rangle^2\right)$$

$$\text{Count rate } I = \Phi N \frac{d^2\sigma}{d\Omega dE_f}\Delta\Omega\Delta E_f$$

$$\frac{d^2\sigma}{d\Omega dE_f} = \frac{\sigma_{coh}}{4\pi\hbar}\frac{k_f}{k_i}S(Q,\omega) + \frac{\sigma_{inc}}{4\pi\hbar}\frac{k_f}{k_i}S_S(Q,\omega)$$

Correlation functions

$$I_S(\vec{Q},t) = \int S_S(\vec{Q},\omega)\exp(i\omega t)d\omega$$

$$G_S(\vec{r},t) = \frac{1}{(2\pi)^3}\int I_S(\vec{Q},t)\exp\left(-i\vec{Q}.\vec{r}\right)d\vec{Q}$$

(similar expressions apply to I and S.)

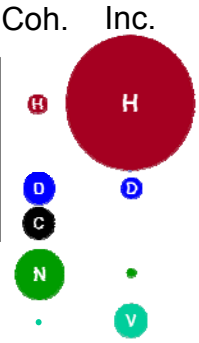

λ	E	v	τ
Å	meV	m/s	μs/mm
1	82	4000	0.25
2	20.5	2000	0.5
4	5.1	1000	1
8	1.3	500	2

What is QENS, and what does it look like?

What is QENS, and what does it look like?

- QENS is inelastic scattering that is almost elastic, centered at zero energy transfer
- There may or may not be associated elastic scattering
- QENS is associated with relaxation phenomena, such as translational diffusion, molecular reorientations, confined motion within a pore, hopping among sites, etc
- Accessible time scales range from fractions of ps to 100s of ns
- Length scales range from Å to 100s of Å
- Most QENS experiments are designed to study incoherent scattering (single particle motions)

Examples of S(Q,ω) data

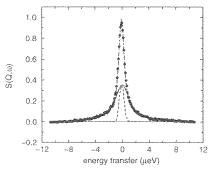

FIG. 2. Quasielastic scattering from water in NaA zeolite at 300 K, $Q = 1.32$ Å^{-1}. The curves are, from top to bottom, the total fitted intensity, the Lorentzian component broadened by resolution, and the shape of the resolution function. Uncertainties due to counting statistics are approximately the size of the symbols.

W.A.Kamitakahara and N. Wada, PRE 77, 041503(2008)

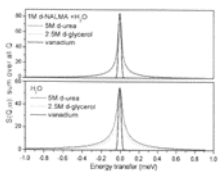

Fig. 2. The incoherent scattering function, summed over Q, for 1 M d-NALMA in H_2O (top) and in pure H_2O (bottom), together with 5 M deuterated urea and 2.5 M deuterated glycerol. The spectra are normalized to the maximum of 2.5 M D-glycerol data.

D. Russo, Chem. Phys. 345,200(2008)

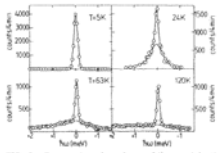

FIG. 5. Temperature dependence of the quasielastic neutron scattering spectrum from $NaNH_2BH_3$. The measurement at 5 K is below the phase transition (19.9 K for the hydrogenated compound) and was used for the determination of the background level.

J. Eckert and W. Press, JCP 73(1)451(1980)

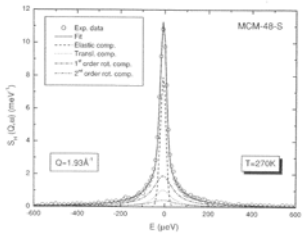

FIG. 2. A typical QENS spectrum from a MCM-48-S hydrated sample at $T = 270$ K, at $Q = 1.93$ Å^{-1}. The errors are no larger than the symbols. The continuous line represents the result of the fit; the dashed line is the elastic component, the dotted, dash-dot, and dash-dot-dot lines represent contributions to the scattering from the first three terms of the Sears expansion.

A. Faraone et al, JCP 119(7)3963(2003)

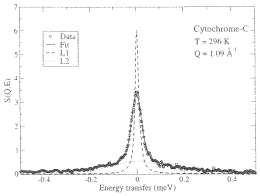

Fig. 7. Measured and calculated spectra for *cytochrome-c* at 296 K, with $Q = 1.09$ Å^{-1}. The experimental data, corrected for scattering from the buffer, are represented as points. The scatter in the points is an indication of their uncertainties. The fitted function (broadened by the instrumental resolution) is shown along with the two unbroadened Lorentzians, L1 and L2.

A.M. Pivovar (unpublished)

More examples of S(Q,ω) data

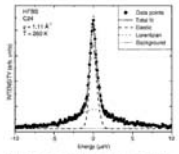

A.D. Enevoldsen et al, JCP 126, 104704 (2007)

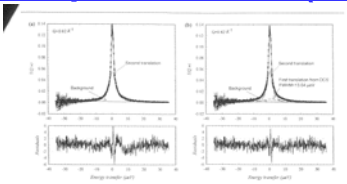

C. Malardier-Jugroot and T. Head-Gordon, PCCP 9, 1962 (2007)

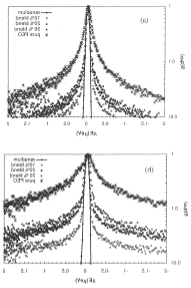

V. Garcia Sakai, J.K. Maranas, et al, Macromolecules, in press.

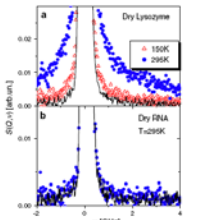

A.P. Sokolov et al, Chem.Phys.345,212(2008)

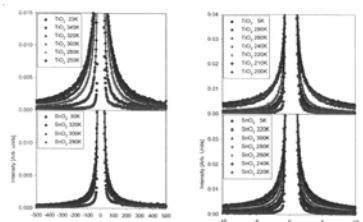

E. Mamontov et al, J.Phys.Chem. C 111, 4328(2007)

American Conference on Neutron Scattering, May 11-15, 2008; QENS Tutorial 17

Typical QENS S(Q,ω)

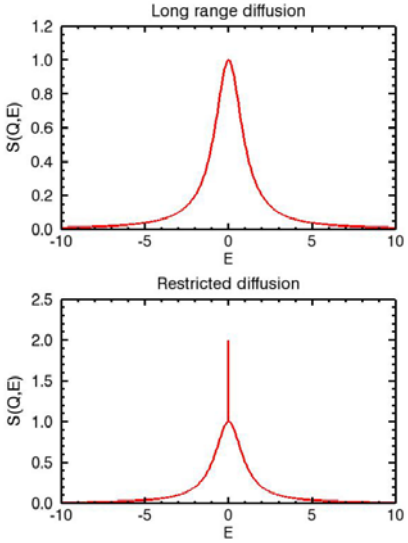

American Conference on Neutron Scattering, May 11-15, 2008; QENS Tutorial 18

Examples of I(Q,t) data

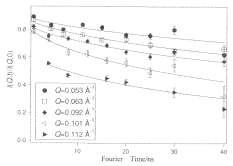

Figure 2. Decay of the normalized intermediate scattering function obtained by NSE against Fourier time at different Q values for DOPC vesicles in D_2O at 60 °C.

M. Nagao et al, Proc. QENS 2006, p. 101 (Mater. Res. Soc. 2007)

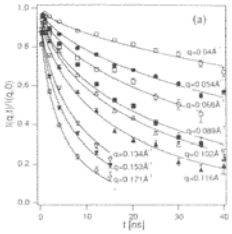

Figure 2: (a) Obtained $I(q,t)/I(q,0)$ at T = 30 according to eq. (1). (b) Semi-logarithmic plot 301.15 K. The solid lines show the existence o

Z.Yi and D.Bossev, Proc. QQENS 2006, p. 123 (Mater. Res. Soc. 2007)

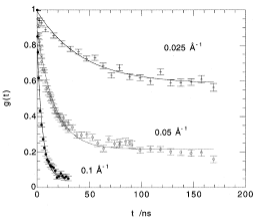

Figure 2. Neutron spin echo decays from a poly(fluorosilicone) gel swollen in acetone at $\varphi = 0.16$ for three different wave-vectors q.

A.-M. Hecht et al, Macromolecules 35, 8552 (2002)

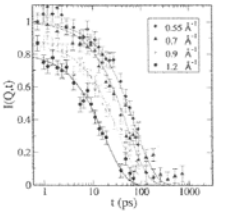

Figure 5. Incoherent intermediate scattering function $I(Q,t)$ obtained by NSE for hectorite clay in the monolayer (top) and bilayer (bottom) states at ambient temperature. Measured Q values are indicated in the legend. Lines correspond to best fits of the data with monoexponentials.

N. Malikova et al, J. Phys. Chem. C 111, 17603 (2007)

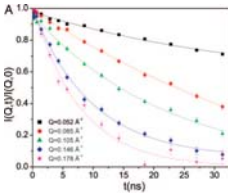

Z. Bu et al, PNAS 102, 17646 (2005)

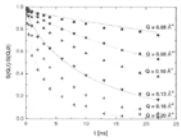

K. Niedzwiedz et al, submitted to Macromolecules (2008)

Typical S(Q,ω) and I(Q,t)

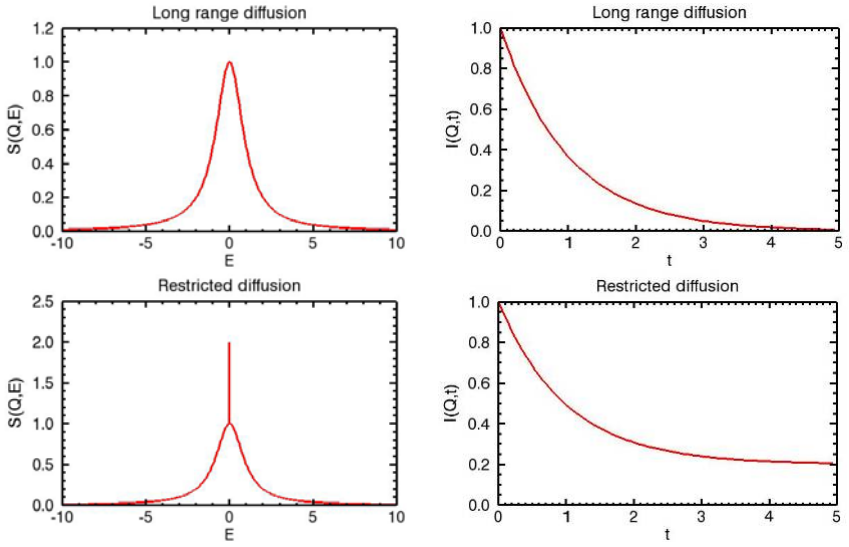

How is QENS measured?

- Triple axis spectrometer (TAS)
- Time-of-flight spectrometer (TOF)
- Backscattering spectrometer (BS)
- Neutron spin echo spectrometer (NSE)

Triple axis spectrometer

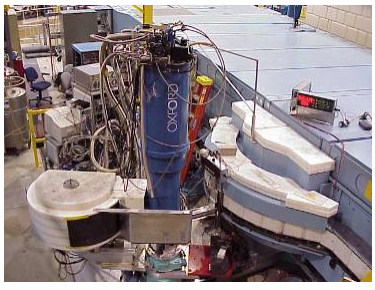

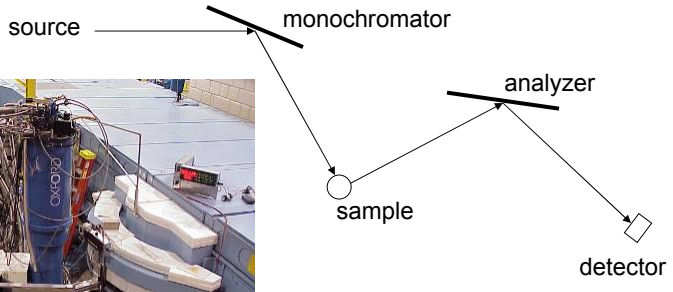

The "SPINS" spectrometer at NIST
Incident energy 14 ~ 2 meV (2.4 ~ 6.1 Å)
Flux at sample: 3.9×10^6 n/cm^2/s at 4 Å.
Resolution: from 0.02 to 1.0 meV

Time-of-flight spectrometer

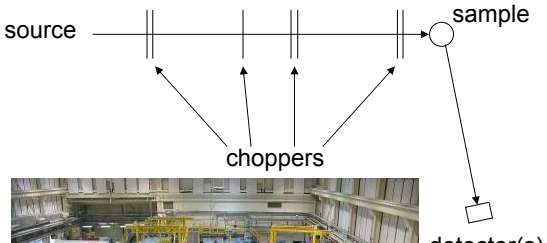

J.R.D. Copley and J.C. Cook,
Chem. Phys. 292, 477 (2003)

The Disk Chopper Spectrometer (NIST)

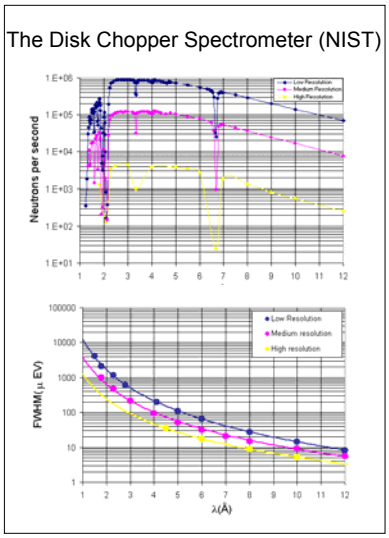

Backscattering spectrometer

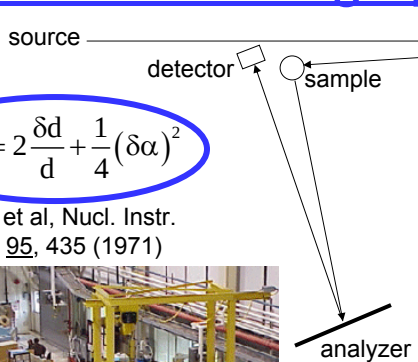

$$\frac{\delta E}{E} = 2\frac{\delta d}{d} + \frac{1}{4}(\delta\alpha)^2$$

M. Birr et al, Nucl. Instr.
Meth. 95, 435 (1971)

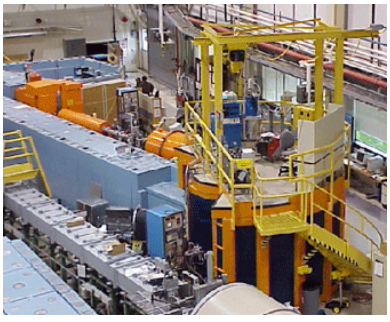

The HFBS Spectrometer (NIST)

Wavelength	6.271 Å
Neutron Energy	2.08meV
Neutron Flux at Sample	3 x 10^5 n cm^{-2} s^{-1}
Energy range	± 36 μeV
Energy resolution at ± 36 μeV	About 1 μeV
Analyzer Span	165°
Q range	0.25 $Å^{-1}$ – 1.75 $Å^{-1}$

A. Meyer, et al, Rev. Sci. Instrum., **74**, 2759 (2003).

Spin echo spectrometer

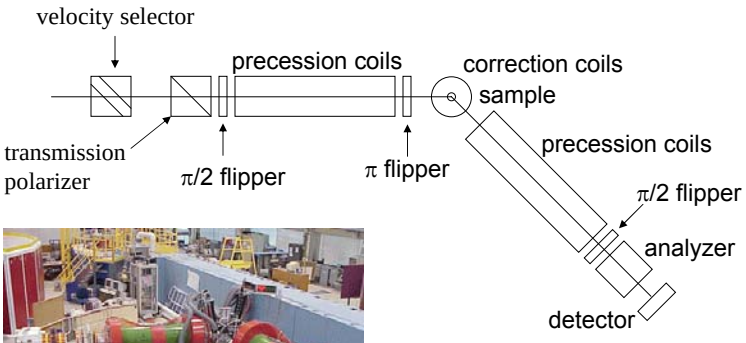

NSE measures I(Q,t) for times t between ≈5 ps and 100-400 ns.

(http://www.ncnr.nist.gov/instruments/nse/)

After D.A. Neumann and B. Hammouda, J. Res. NIST 98, 89 (1993)

Spin echo spectrometer

IN WORDS

The spin echo technique uses the precession of a neutron's magnetic moment (spin) in a magnetic field as a "clock" to measure the neutron's speed.

The neutron spins undergo many (of order 10^5) turns in the precession coils.

In effect each spin is "wound up" in the first coil and "unwound" by the same amount in the second coil when the scattering is elastic.

If the scattering is inelastic, the "winding up" and "unwinding" processes do not completely cancel. The polarization of the neutron beam at the echo position is a measure of the inelasticity of the scattering.

IN EQUATIONS

$$\phi = \gamma \frac{J_0}{v_0} \quad (J_i = \int B_i dl) \quad (\omega_L = \gamma B)$$

$$\left[\gamma = 1.83247185(43)\times 10^8 \text{ rad/s/T}\right]$$

$$\Delta\phi = \gamma \frac{J_0}{v_0} - \gamma \frac{J_1}{v_1} \approx \gamma \frac{J_0}{v_0}\left(\frac{\delta v}{v_0}\right) - \gamma \frac{\delta J}{v_0}$$

At the echo condition δJ vanishes.

$$\hbar\omega = \tfrac{1}{2} m\delta\left(v_0^2\right) = m v_0 \delta v \,;\, v_0 = \frac{h}{m\lambda}$$

$$\Delta\phi \approx \gamma \frac{J_0}{v_0^2}\frac{\hbar\omega}{m v_0} = t_F\omega \;;\; t_F = \gamma \frac{J_0 \hbar}{m v_0^3}$$

$$P_x = \left\langle \cos(\Delta\phi) \right\rangle \;;\; t_F = \gamma \frac{m^2}{2\pi h^2} J_0 \lambda^3$$

$$= \frac{\int S(Q,\omega)\cos(t_F\omega)\,d\omega}{\int S(Q,\omega)\,d\omega} = \frac{I(Q,t_F)}{I(Q,0)}$$

Comparison of spectrometers

• **Resolution**
TAS → TOF → BS → NSE
Good → Very good → Excellent

• **Q and ω coverage**
TOF has wide coverage in Q and ω, BS has wide Q coverage (but poor Q resolution), TAS/NSE are more restricted. BS has restricted ω range.

• **Coherent and incoherent scattering**
NSE is best suited to measurements of coherent diffusive or dispersionless excitations at long times. Other forms of dynamical behavior (in the same time range) can be studied, but they are less straightforward.

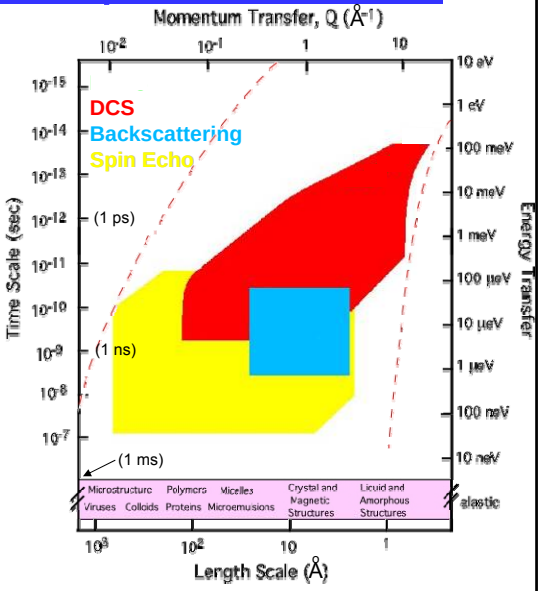

How is QENS modeled?

Separation of motions with different time scales
Vibrations (internal, external), translations
Local motions (local diffusion, reorientations)
Translational diffusion

It is generally assumed that motional time scales differ so much that the coupling between different types of motion can be neglected.
For example, consider vibrations and diffusion :

$$I(Q,t) = I_V(Q,t) \cdot I_D(Q,t)$$
$$S(Q,\omega) = S_V(Q,\omega) \otimes S_D(Q,\omega)$$

In this case the approximation is justified. On the other hand an equivalent approximation, separating translational and rotational diffusive motions, is less satisfactory.

Detailed balance and moment rules

S(Q,ω) should ideally satisfy detailed balance and the moment sum rules.

Detailed balance

$$S(Q,-\omega) = e^{-\hbar\omega/k_B T}\, S(Q,\omega)$$

Most model S(Q,ω)'s do not satisfy these rules.

Moments

$$\langle\omega^0\rangle = \int_{-\infty}^{\infty} S(Q,\omega)\,d\omega = 1$$

$$\langle\omega^1\rangle = \int_{-\infty}^{\infty} \omega S(Q,\omega)\,d\omega = \frac{\hbar Q^2}{2M}$$

$$\langle\omega^2\rangle = \int_{-\infty}^{\infty} \omega^2 S(Q,\omega)\,d\omega \approx \frac{Q^2 k_B T}{M}$$

At sufficiently large Q and ω the ideal gas scattering function applies.

$$S_{IG}(Q,\omega) = \frac{1}{\sqrt{2\pi}\,\sigma}\exp\left[\frac{-(\omega-\Delta)^2}{2\sigma^2}\right] \text{ with } \Delta = \frac{\hbar Q^2}{2M},\ \sigma = \sqrt{\frac{Q^2 k_B T}{M}}$$

$$= \frac{1}{\sqrt{2\pi}\,\sigma}\exp\left[\frac{-\Delta^2}{2\sigma^2}\right]\exp\left[\frac{-\omega^2}{2\sigma^2}\right]\exp\left[\frac{\hbar\omega}{2k_B T}\right]$$

$S_{IG}(Q,\omega)$ is Gaussian: unit area, width ∝ Q, shift ∝ Q^2

Popular models

Long range continuous diffusion

$$I(Q,t) = \exp\left(-DQ^2 t\right)$$

and S(Q,ω) is a Lorentzian:

$$S(Q,\omega) = \frac{1}{\pi}\frac{\Delta\omega(Q)}{\omega^2 + \left[\Delta\omega(Q)\right]^2}$$

with $\Delta\omega(Q) = DQ^2$

Long range jump diffusion

(G.T.Chudley and R.J. Elliott, Proc. Phys. Soc. 77, 353 (1961))

S(Q,ω) is a Lorentzian with

$$\Delta\omega(Q) = \frac{1}{Z\tau}\sum_{j=1}^{Z}\left(1-\exp\left[-\mathbf{Q}\cdot\mathbf{s}_j\right]\right) \quad \text{(lattice)}$$

$$\Delta\omega(Q) = \frac{6D_s}{r^2}\left(1-j_0[Qr]\right) \quad \text{(isotropic)}$$

Spatially confined continuous diffusion on a sphere, radius r

(V.F. Sears, Can. J. Phys. 44, 1999 (1966))

$$S(Q,\omega) = j_0^2(Qr)\,\delta(\omega) + \sum_{\ell=1}^{\infty} j_\ell^2(Qr)\times$$

$$\times(2\ell+1)\frac{1}{\pi}\frac{\ell(\ell+1)D_R}{\left[\ell(\ell+1)D_R\right]^2 + (\hbar\omega)^2}$$

Spatially confined jump diffusion

(2 sites, separation d)

$$I(Q,t) = A_0(Q) + \left[1-A_0(Q)\right]\exp(-2t/\tau)$$

$$S(Q,\omega) = A_0(Q)\,\delta(\omega) + \left[1-A_0(Q)\right]\frac{1}{\pi}\frac{\Gamma}{\omega^2+\Gamma^2}$$

$A_0(Q) = \frac{1}{2}\left[1+j_0(Qd)\right]$, Γ independent of Q

The Elastic Incoherent Structure Factor (EISF)

$$S(Q,\omega) = A_0(Q)\delta(\omega) + S_{inel}(Q,\omega)$$

$$\int_{-\infty}^{\infty} S(Q,\omega)\,d\omega = 1 \qquad A_0(Q) = I(Q,\infty) = \frac{1}{2\pi}\int_{-\infty}^{\infty} G(r,\infty)\exp(-iQ\cdot r)\,dr$$

$$A_0 = \frac{\text{elastic}}{\text{elastic} + \text{inelastic}} \qquad A_0(Q) = \frac{1}{N^2}\left|\sum_j \exp(iQ\cdot r_j)\right|^2$$

See, e.g., Yildirim et al, PRB 60, 314, (1999).

- For long-range diffusion A_0=0 (except at Q=0)
- For both long-range and restricted diffusion A_0 = 1 at Q=0
- For a continuous set of sites $A_0 \rightarrow 0$ at large Q
- For a discrete set of sites $A_0 \rightarrow$ >0 at large Q, e.g. $A_0 \rightarrow 1/N$ for N equivalent sites.

Spatially confined jump diffusion

(1) Jumps among 2 sites (site separation d)

τ is average time between jumps

$$S(Q,\omega) = \frac{1}{2}\left[1 + j_0(Qd)\right]\delta(\omega) + \frac{1}{2}\left[1 - j_0(Qd)\right]\frac{1}{\pi}\left(\frac{2\tau}{4+\omega^2\tau^2}\right)$$

(2) Jumps among 3 sites on a circle of radius r

$$S(Q,\omega) = \frac{1}{3}\left[1 + 2j_0\left(Qr/\sqrt{3}\right)\right]\delta(\omega) + \frac{2}{3}\left[1 - 2j_0\left(Qr/\sqrt{3}\right)\right]\frac{1}{\pi}\left(\frac{3\tau}{9+\omega^2\tau^2}\right)$$

(3) Jumps among N sites on a circle of radius r

$$S(Q,\omega) = A_0(Q)\delta(\omega) + \sum_{\ell=1}^{N} A_\ell(Q)\frac{1}{\pi}\left(\frac{\tau_\ell}{1+\omega^2\tau_\ell^2}\right) \qquad \tau_\ell^{-1} = 2\tau^{-1}\sin^2\left(\frac{\pi\ell}{N}\right)$$

$$A_\ell(Q) = \frac{1}{N}\sum_{n=1}^{N} j_0(Qr_n)\cos\left(\frac{2\ell n\pi}{N}\right) \qquad r_n = 2r\sin\left(\frac{n\pi}{N}\right)$$

Examples of EISFs and widths

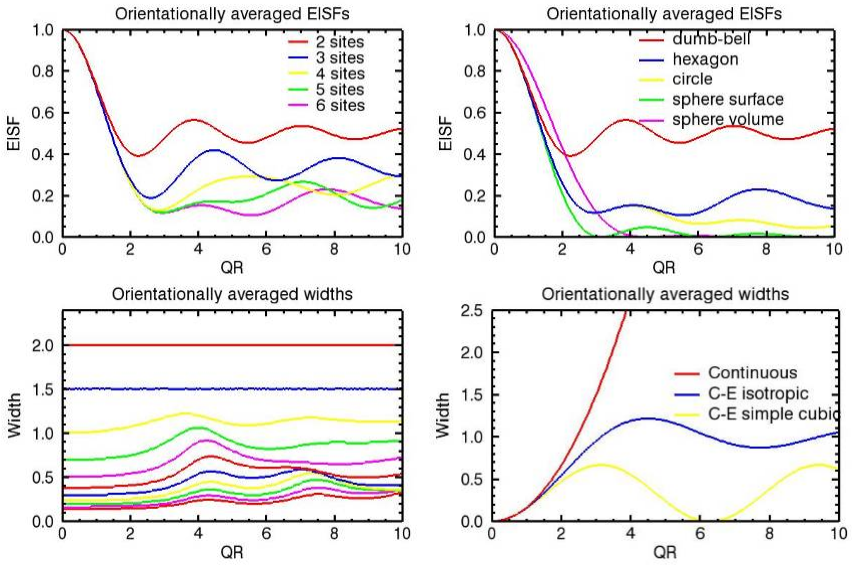

Practicalities ("caveat utor")

- **Planning an experiment**
  - Choice of spectrometer: match instrument/instrument setup (e.g. choice of wavelength) to time scale(s) of interest
  - Choice of sample shape: typically annular for TOF and BS - flat plate for TAS and NSE
    - Both geometries can be challenging, esp. annular powders, since optimum thicknesses are of order tenths of a mm
  - Choice of sample dimensions (consider self-shielding, multiple scattering)

Choice of spectrometer

Matching the instrument to time scale(s) of interest

← (slow) ——— S(Q,ω) ——— (fast) →

Resolution ↕

	delta-function peak	Narrow peak	Medium width peak	Broad peak	Flat back-ground
Low resn. (broad)	(Elastic)	**Elastic**	**Elastic**	**Match**	(Flat)
Med. resn. (medium)	(Elastic)	**Elastic**	**Match**	**Flat**	(Flat)
High resn. (narrow)	(Elastic)	**Match**	**Flat**	**Flat**	(Flat)

Multiple scattering and self-shielding

- For slab geometry self-shielding (SS) depends strongly on orientation; for annular geometry it is almost isotropic

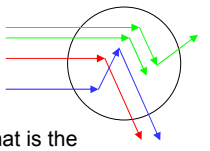

- The 90% transmission "rule of thumb"
  - The "rule" is that if T=90%, S_1=10% and S_m/S_1=10%, and if that is the case multiple scattering (MS) can be neglected.
  - The first part is valid for slab geometry, not necessarily valid for other geometries: for example, consider annular geometry with b=0.1 mm and R=10 mm, i.e. b/R = 0.01; if T=90%, S1=8.5% and $S_m/S_1 \approx$ 18%.
  - If indeed S_m/S_1 = 10%, can neglect of MS be justified? What if S_m/S_1 = 15%?

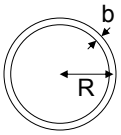

- If T is calculated what value should be used for σ_s?
  - In general σ_s depends on E_i, T, chemistry, morphology, … See J.R.D. Copley, Neutron News, 18(1), 30 (2007).
- An excellent reference for MS/SS is V.F. Sears, Adv. Phys. 24, 1 (1975).

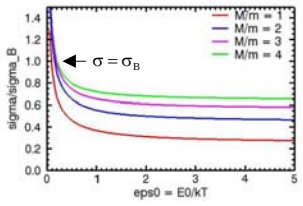

Multiple scattering

Quotes from early papers

"The average of distributions obtained at small angles of scattering (Q<1.4) was taken to be the multiple scattering component, …"

"The thickness of the water films ranged from 0.01 inches (~0.08 M.F.P.) to 0.035 inches (~0.3 M.F.P.) depending on the amount of multiple scattering which could be tolerated. ... Multiple scattering was estimated roughly [ref.] as shown ..."

Quotes from more recent papers

"Sample thicknesses were kept around 0.2 mm to achieve transmissions of ≈ **90 %** and avoid multiple scattering effects."

"The sample thickness was chosen to ensure **90%** neutron transmission and thus minimize multiple scattering effects."

"… sample holders chosen to ensure greater than **90%** neutron beam transmission through the sample in order to minimize the effects of multiple scattering …"

"The multiple scattering was minimized using a small thickness for the sample, which was also confirmed by a transmission higher than **0.9**."

"Total neutron scattering from the samples was ~**10%**; thus, multiple scattering was negligible, …"

Total scattering cross sections

- Total scattering cross sections vary with incident energy, temperature, morphology, and chemical environment (not just chemical composition)
- Total scattering cross sections vary as 1/v at sufficiently long wavelengths (as do absorption cross sections)

$$\sigma_S(E_0) = \int_{4\pi}\int_0^{\infty}\left(\frac{d^2\sigma}{d\Omega dE_f}\right)dE_f d\Omega$$

$$\propto \frac{1}{E_0}\int_{KAR(E_0)} S(Q,\omega)\,Q dQ d\omega$$

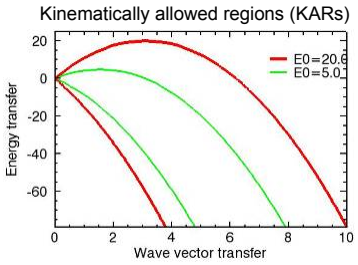

International Conference

Nuclear Energy for New Europe 2004

Portorož • Slovenia • September 6-9

port2004@ijs.si
www.drustvo-js.si/port2004
+386 1 588 5247, fax +386 1 561 2276
PORT2004, Nuclear Society of Slovenia, Jamova 39, SI-1000 Ljubljana, Slovenia

On the Thermal Scattering Law Data for Reactor Lattice Calculations
A. Trkov and M. Mattes

Total neutron scattering cross section of water

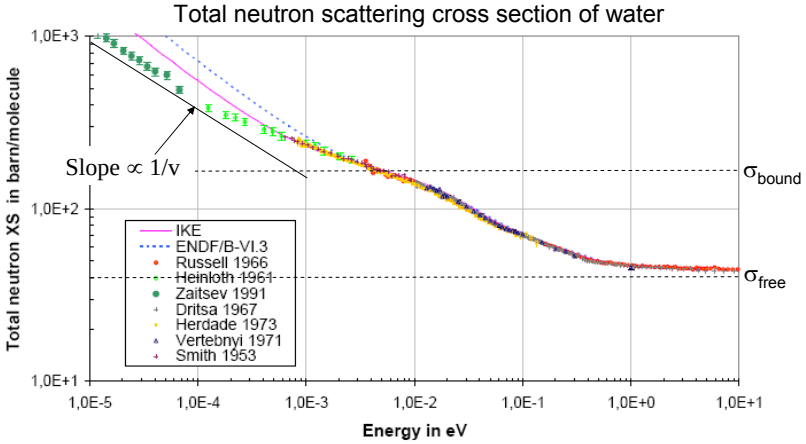

Practicalities (contd.)

- **Performing the experiment**
  - What to run, apart from the sample(s), and how to divide the time?
    - Empty can? Empty cryostat/CCR?
    - Elastic scatterer (for detector efficiencies, normalization, resolution)?
    - Time-independent background ("dark count")?
  - Choices of wavelength, resolution, dynamic range etc.
- **Data treatment ("postparation")**
  - The options available for data treatment depend on how the experiment was planned and performed.
  - Keep in mind:
    - the resolution-limited "elastic" scattering may include elastic scattering from host material in the sample, and other sources, as well as QENS due to motions too slow to be distinguished from truly elastic scattering
    - The flat "background" may include true background as well as QENS from motions too fast to be detected as such
  - When subtracting the empty can, consider the attenuating effect of the sample

Examples of QENS

- Water
- Cubane
- Liquid lead
- C_{60}

Liquid water

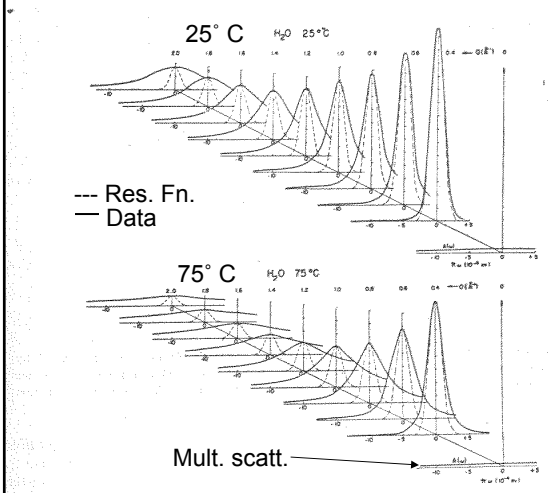

Fig. 1. The scattering function $S(Q,\omega)$ for water (a) at 25°C and (b) at 75°C for small values of $\hbar\omega$. The energy resolution functions are shown as dashed curves. The multiple scattering $A(\omega)$ which was subtraced is also shown.

M. Sakamoto et al, Proc. Int. Conf. Magn. and Cryst. 1961, vol. II; J. Phys. Soc. Japan **17**, Suppl. B-II, 370 (1962).

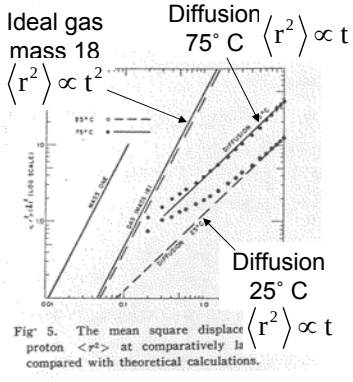

Fig. 5. The mean square displace proton $\langle r^2 \rangle$ at comparatively la compared with theoretical calculations.

Cubane, C_8H_8

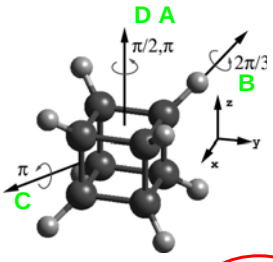

Phase transition, from orthorhombic (α=73°) to orthorhombic (α=103°) at 394K.
Melting at 405K

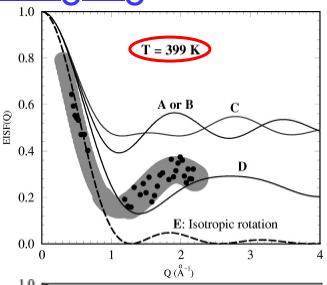

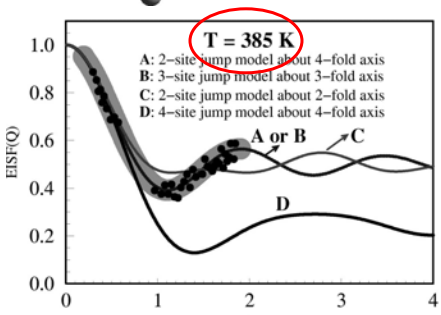

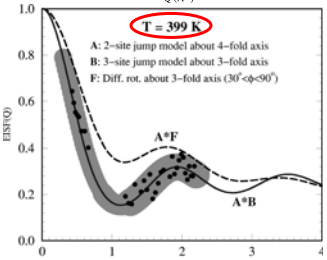

T. Yildirim et al, PRB 60, 314 (1999)

Liquid lead

S(Q,ω)

B.N.Brockhouse and N.K.Pope, PRL 3, 259(1959)

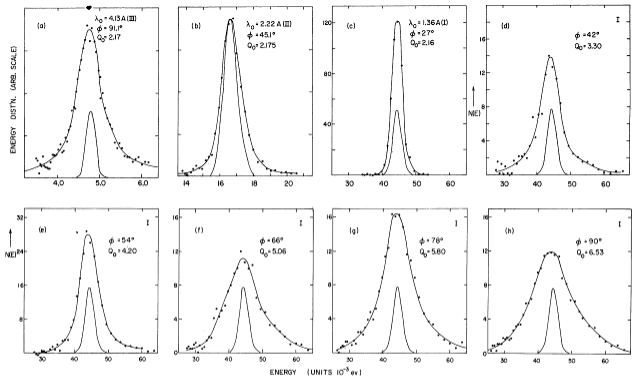

FIG. 1. A selection of energy distributions of neutrons scattered from liquid lead at 620°K, each with its resolution function (appropriate to the incident energy). All patterns have been corrected for background, for container scattering, for instrument sensitivity, and all except (a) for multiple scattering. [Figure 1 (a) is thought to contain ~ 10 % multiple scattering.] The factor k'/k_0 of Eq. (1) has also been removed. Figures 1 (a), (b), and (c) show energy distributions obtained under different resolutions at the main diffraction peak. In Fig. 1 (b) the resolution function has been normalized at the peak to illustrate the energy broadening. Figures 1 (a) and (b) are in agreement that the half-width at half maximum of the distribution is $\sim 3.5 \times 10^{-4}$ ev, compared with the 8×10^{-4} ev expected on simple arguments of diffusion broadening by small motions [references 2 and 3]. The shape is roughly Lorentzian. Figures (c) to (h) show Series I distributions at different values of Q_0. The intensities are consistently normalized but note the different ordinate scales.

Liquid lead

I(Q,t)

G(r,t)

(times t in 0.1ps)

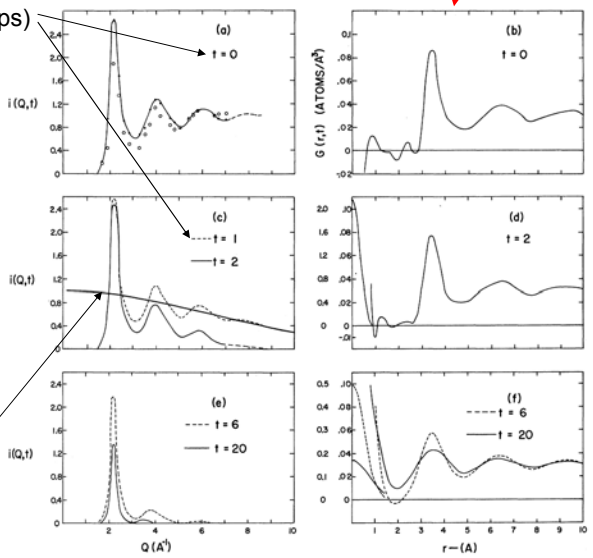

FIG. 2. A selection of smoothed curves of $i(Q,t)$ vs Q, and curves of $G(r,t)$ vs r for values of $t = 0$, 1, 2, 6, and 20×10^{-13} sec. The closed circles in Fig. 2(a) show the experimental points for the integrated intensities $i(Q, 0)$ of Series I. The open circles in Fig. 2(a) are values of $i(Q, 0)$ calculated following Eq. (4). Note that the left-hand scales in Figs. 2(d) and 2(f) apply to the self-correlation functions.

Ideal gas

Buckminsterfullerene, C_{60}

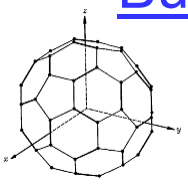

An orientational order-disorder phase transition occurs at ≈255K

N.B. Jumps among equivalent orientations produce no (coherent) intensity.

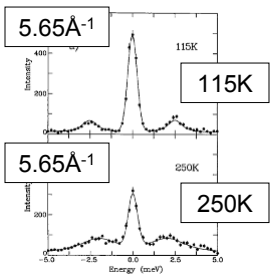

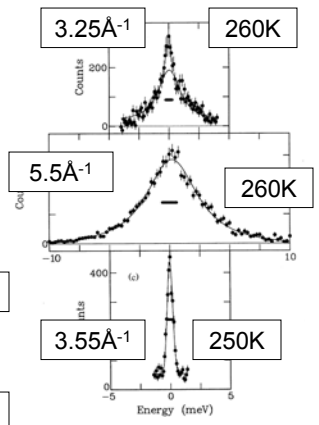

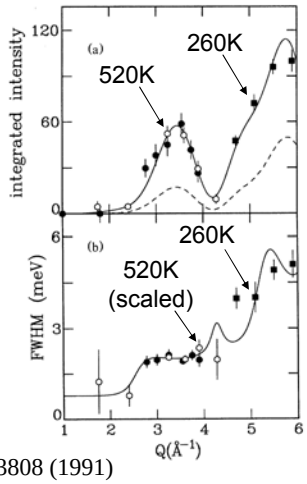

D.A. Neumann et al, PRL 67, 3808 (1991)
D.A.Neumann et al, JCP 96, 8631 (1992)

Further reading

- M. Bée, “Quasielastic Neutron Scattering … in Solid State Chemistry, Biology and Materials Science” (Adam-Hilger, Bristol 1988) (but difficult to find)
- R. Hempelmann, “Quasielastic Neutron Scattering and Solid State Diffusion” (OUP, Oxford and New York, 2000)
- J.S. Higgins and P. Benoit, “Polymers and Neutron Scattering” (OUP, Oxford and New York, 2000)
- J. Fitter, T. Gutberlet, and J. Katsaras, eds., “Neutron Scattering in Biology” (Springer, Berlin, 2006)
- Proceedings of QENS conferences (next slide)

Recent QENS Conferences/Proceedings

- **QENS 1992, 1994, 1996, 1998,…**
- **QENS 2000:** Physica B: 301, Issues 1-2, July 2001
- **QENS 2002:** Chemical Physics 292, Issues 2-3, (2003)
- **QENS 2004:** Phys. Chem. Chem. Phys. 7 (2005); go to http://blake.ism.u-bordeaux1.fr/A.Desmedt/qens2004.html
- **QENS 2006:** “Quasi-Elastic Neutron Scattering Conference 2006 (QENS2006)”, ed. P.E. Sokol, H. Kaiser, D. Baxter, R. Pynn, D. Bossev, M. Leuschner (Mat. Res. Soc., Warrendale, PA, 2007)
- **QENS 2009:** to be held 2/10-13/09 at the Paul Scherrer Institut, Switzerland.